

**Mitochondria-Targeting NIR Fluorescent Potassium Ion Sensor:  
Real-Time Investigating Mitochondrial K<sup>+</sup> Regulation of  
Apoptosis *in Situ***

Guangjie Song,<sup>ab</sup> Di Jiang,<sup>b</sup> Lei Wang,<sup>a</sup> Juewei Ning,<sup>a</sup> Xiangzhong  
Sun,<sup>a</sup> Fengyu Su,<sup>\*c</sup> Meiwan Chen<sup>\*b</sup> and Yanqing Tian<sup>\*a</sup>

## **1. Experimental section**

1.1 Reagents and solvents

1.2 Instruments

1.3 Synthesis of **TAC-Rh**

1.4 Cell lines

1.5 Colocalization test of **TAC-Rh** and Mito-Tracker Green

1.6 Monitoring the intracellular  $K^+$  efflux using **TAC-Rh** and cell apoptosis

1.7 Cytotoxicity of **TAC-Rh**

**2. Table S1** Representative structures and some parameters of  $K^+$  fluorescent probes

## **3. Figure section**

Fig. S1  $^1H$  NMR of **TAC-Rh**

Fig. S2 HRMS of **TAC-Rh**

Fig. S3 UV titration spectra of **TAC-Rh**

Fig. S4 pH influence

Fig. S5 Reaction kinetics of **TAC-Rh**

Fig. S6 Selectivity to  $K^+$  of **TAC-Rh**

Fig. S7 Interference of other metal ions

Fig. S8 MTT assay for **TAC-Rh**

Fig. S9-S19 Time-dependent confocal fluorescence microscopy imaging of **TAC-Rh**-stained cells

Fig. S20 Confocal fluorescence microscopy imaging stimulated with  $H_2O_2$

Fig. S21 Confocal fluorescence microscopy imaging in 80 mM KCl

## Experimental Section

### 1.1 Reagents and solvents.

All reagents were purchased from commercial sources and used without further purification. The solutions of metal ions were prepared from deionized water. All the measurement samples were prepared from deionized water at room temperature.

### 1.2 Instruments.

<sup>1</sup>H NMR spectrum measurement was operated on high performance digital FT-NMR spectrometer AVANCE 600III, Bruker, using CDCl<sub>3</sub> as solvent. HRMS spectrum was obtained on Thermo LTQ Orbitrap XL Mass Spectrometer. UV-vis spectra were measured utilizing a PerkinElmer Lambda 25 UV/Vis spectrophotometer. Fluorescence measurements were performed on a Horiba FluoroMax-4 spectrofluorophotometer. And confocal images were photographed by Leica TCS SP8 confocal laser scanning microscope system.

### 1.3 Synthesis of *TAC-Rh*.

**9-(2-Carboxyphenyl)-6-(diethylamino)-1,2,3,4-tetrahydroxanthylum (compound 1)** and **TAC-CHO** were synthesized as described previously in literature.<sup>[1,2]</sup>

**TAC-CHO** (0.32 g, 0.45 mmol) and **Compound 1** (0.21 g, 0.45 mmol) were dissolved in acetic oxide (5 mL). Then the reaction mixture was heated at 90°C and stirred for 8 h under nitrogen atmosphere. After cooled down to room temperature and following solvent evaporation under reduced pressure, the mixture was purified by column chromatography (silica gel, dichloromethane/methanol = 100:1, v:v). 0.24 g (0.20 mmol) of blue solid (**TAC-Rh**) was obtained, yield: 46.1 %.<sup>[2]</sup> <sup>1</sup>H NMR (CDCl<sub>3</sub>, 600

MHz),  $\delta$  (ppm) = 8.08-8.22 (m, 1H), 7.81-7.94 (m, 1H), 7.69-7.51 (m, 13H), 4.53-4.69 (m, 6H), 4.22-4.33 (m, 3H), 4.07-4.16 (m, 2H), 3.29-3.81 (m, 34H), 3.01-3.16 (m, 4H), 2.74-2.91 (m, 2H), 1.96-2.09 (m, 2H), 1.61-1.78 (m, 3H), 0.73-1.01 (m, 5H). Calcd. [M-I]<sup>+</sup>: 1079.5740; found value [M-I]<sup>+</sup>: 1079.5729.

#### *1.4 Cell lines*

HeLa, MDA-MB-231 and MCF7 cells (American Type Culture Collection, ATCC, ManassasVA) were cultured in Dulbecco's Modified Eagle Medium (DMEM) supplemented with 10% fetal bovine serum, 100 u/ml penicillin, 100  $\mu$ g/mL streptomycin and incubated at 37°C in 5% CO<sub>2</sub> atmosphere.

#### *1.5 Colocalization test of TAC-Rh and Mito-Tracker Green*

Colocalization analysis was performed in HeLa cells using Mito-Tracker Green dye. Cells were first internalized with **TAC-Rh** (3  $\mu$ M in cell culture medium) for 30 min. Then, Mito-Tracker Green diluted in the fresh medium was added into the wells to stain cells for 45 min at 37°C. The resulting concentration of Mito-Tracker Green in the cell medium was 40 nM. After washed with PBS for 3 times, the CLSM images were photographed by a Leica TCS SP8 confocal laser scanning microscope system. , Excitation filter: 638 nm for **TAC-Rh**, 488 nm for Mito-Tracker Green; Emission: 650-750 nm for **TAC-Rh**, 500-550 nm for Mito-Tracker Green.

#### *1.6 Monitoring the intracellular K<sup>+</sup> efflux using TAC-Rh and cell apoptosis*

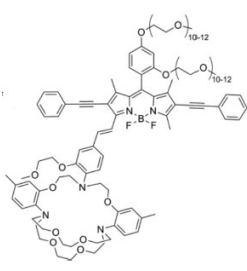
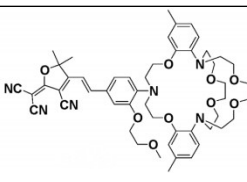
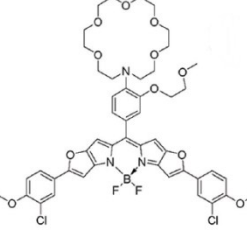
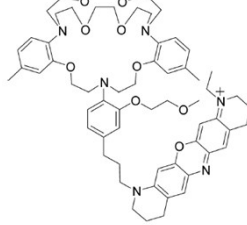
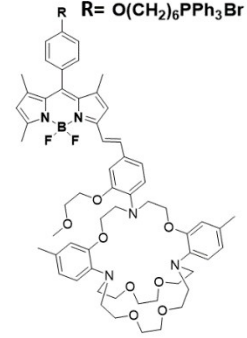
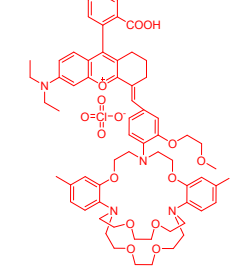
HeLa cells or MCF7 cells were seeded in confocal petri dishes with  $1.5 \times 10^4$  cells per dish respectively, and incubated overnight at 37°C. On the following day, the cells were internalized with **TAC-Rh** (3  $\mu$ M) for 30 min at 37°C. And then 5  $\mu$ L Annexin V/FITC

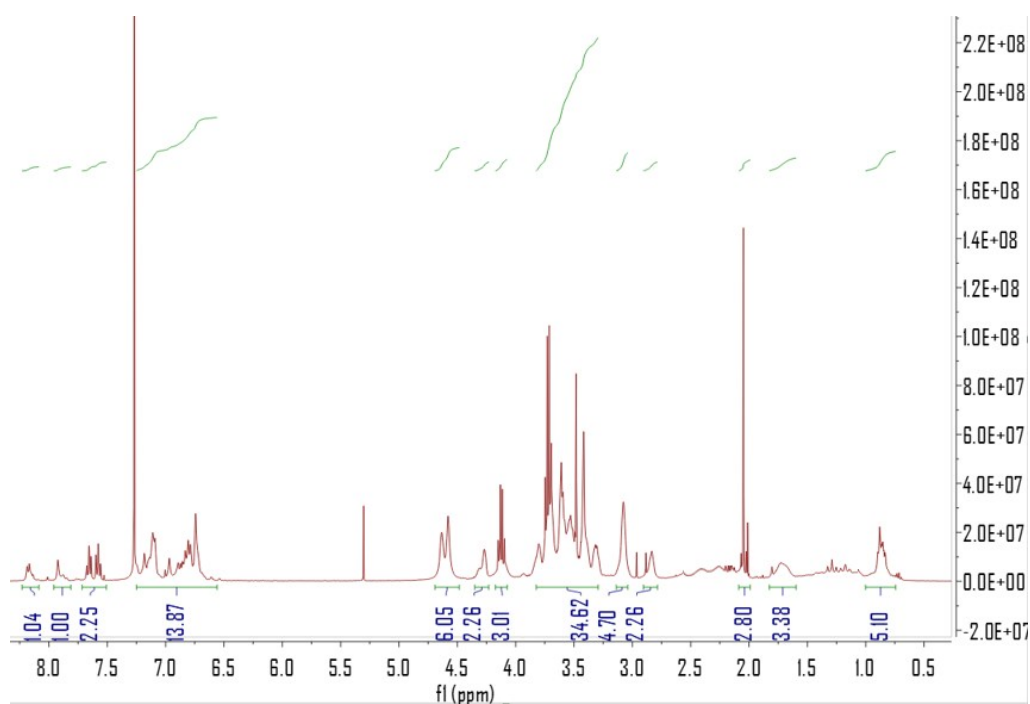
and 10  $\mu$ L propidium iodide were subsequently added on the basis of the protocol when apoptosis analysis was needed. Fluorescence changes in cells after different treatments (including 10  $\mu$ M ionomycin/nigericin, 80 mM KCl and 10  $\mu$ M ionomycin and 100  $\mu$ M  $H_2O_2$ ) were visualized by Leica TCS SP8 confocal laser scanning microscope system. Excitation filter: 488 nm for Annexin V/FITC, 552 nm for PI, 638 nm for **TAC-Rh**; Emission: 493-540 nm for Annexin V/FITC, 600-650 nm for PI, 650-750 nm for **TAC-Rh**.

### *1.7 Cytotoxicity of TAC-Rh*

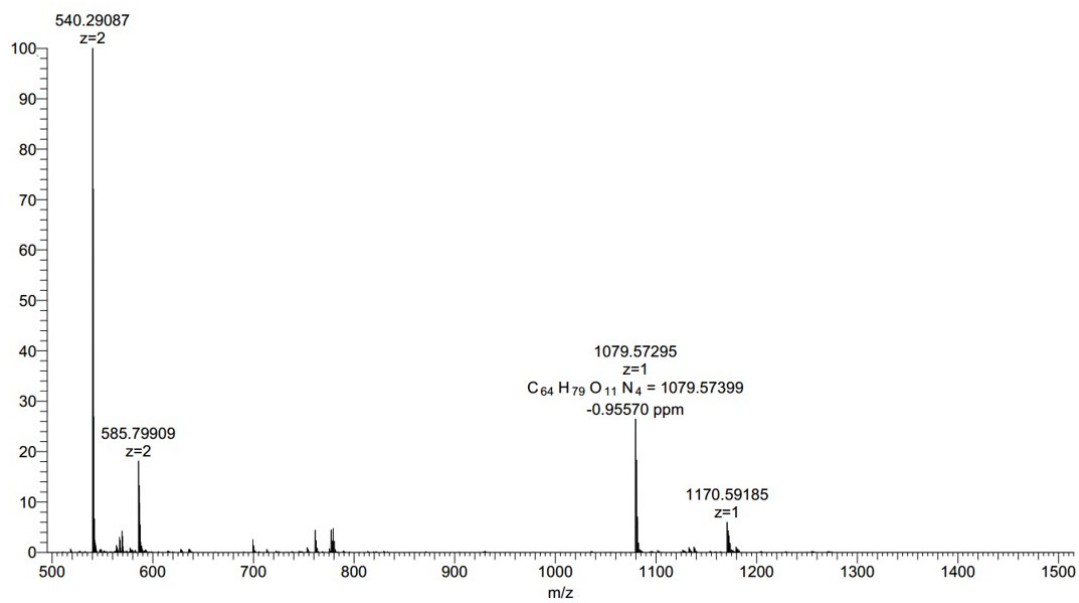
Colorimetric MTT metabolic activity assay was used to determine cell viability. HeLa, MCF7 and MDA-MB-231 cells ( $5 \times 10^3$  cells/well) were respectively cultured in 96-well plates at 37 °C, and exposed to varying concentrations for 1, 2, 3 and 6 h. Cells treated with medium only served as a negative control group. After removing the supernatant of each well and washing by PBS, 100  $\mu$ L of medium containing MTT were then introduced. After incubation for another 4 h, the resultant formazan crystals were dissolved in 100  $\mu$ L DMSO and the absorbance intensity measured by a microplate reader (SpectraMax M5, Molecular Devices, USA) at 490 nm. All experiments were performed in triplicate, and the relative cell viability (%) was expressed as a percentage relative to the untreated control cells.

Table S1 Representative structures and some parameters of K<sup>+</sup> fluorescent probes

type	No.	Structure	Ex/Em (nm)	Stokes shifts	Ref.
NIR	4		617/650	33 nm	3
			561/650	89 nm	4
			670/688	18 nm	5
			620/680	60 nm	6
Mitochondria-Targeting	1	<p>R = O(CH<sub>2</sub>)<sub>6</sub>PPH<sub>3</sub>Br<sup>+</sup></p> 	540/570	30 nm	2
<b>NIR and Mitochondria-Targeting</b>	<b>This work</b>		<b>600/720</b>	<b>120 nm</b>	



**Figure S1.**  $^1\text{H}$  NMR of TAC-Rh.



**Figure S2.** HRMS of TAC-Rh.

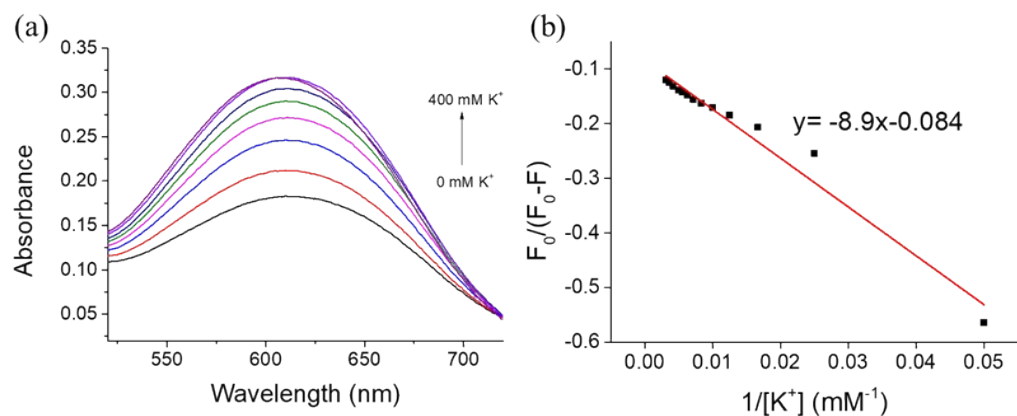


**Figure S3.** (a) UV-Vis absorption spectra of **TAC-Rh** (10 mM) during the titration in Tris buffer (pH = 7.4; 5.0mM)/CTAB (0.5 mM) solution from 0 mM to 400 mM  $K^+$ , (b) Benesi-Hildebrand plot for **TAC-Rh** by referring the Figure 2a in the manuscript text.

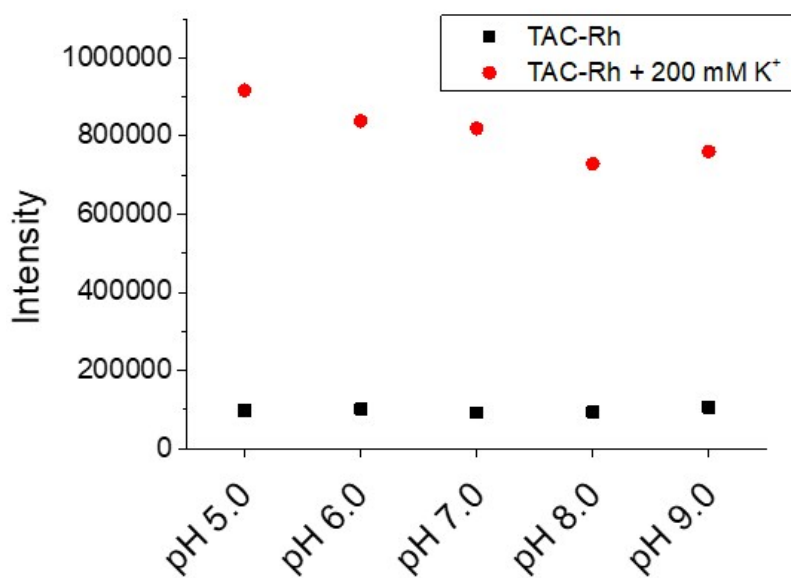


**Figure S4.** Fluorescence intensity at 720 nm of **TAC-Rh** (10  $\mu$ M) without or with  $K^+$  (200 mM) in HEPES buffer (5.0 mM)/CTAB (0.5 mM) solution at different pH.

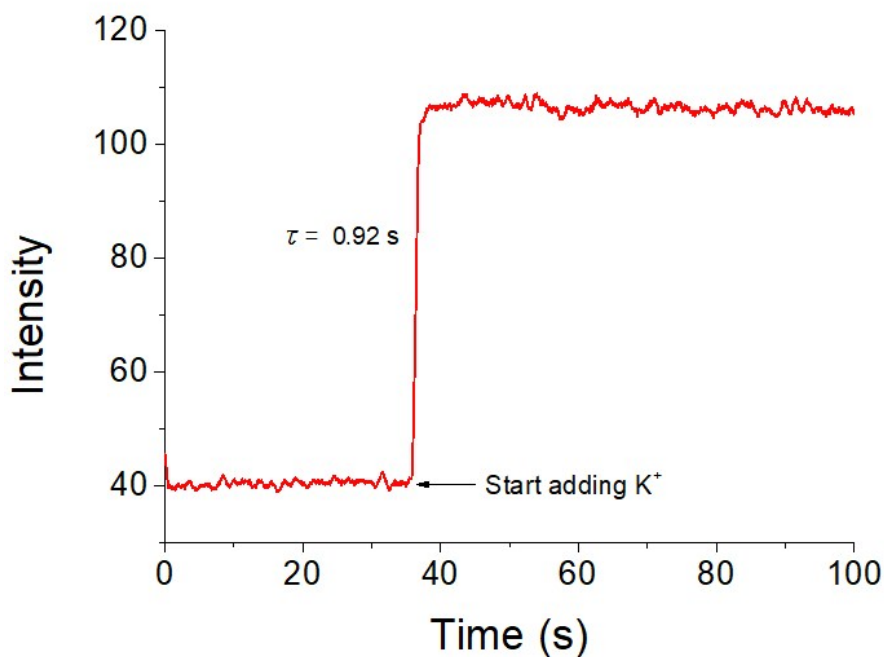


**Figure S5.** Reaction kinetics of **TAC-Rh** observed at 720 nm in the absence and presence of  $\text{K}^+$  in HEPES buffer (pH 7.4, 5.0 mM)/CTAB (0.5 mM) solution. Kinetic data were collected every 0.1 seconds.

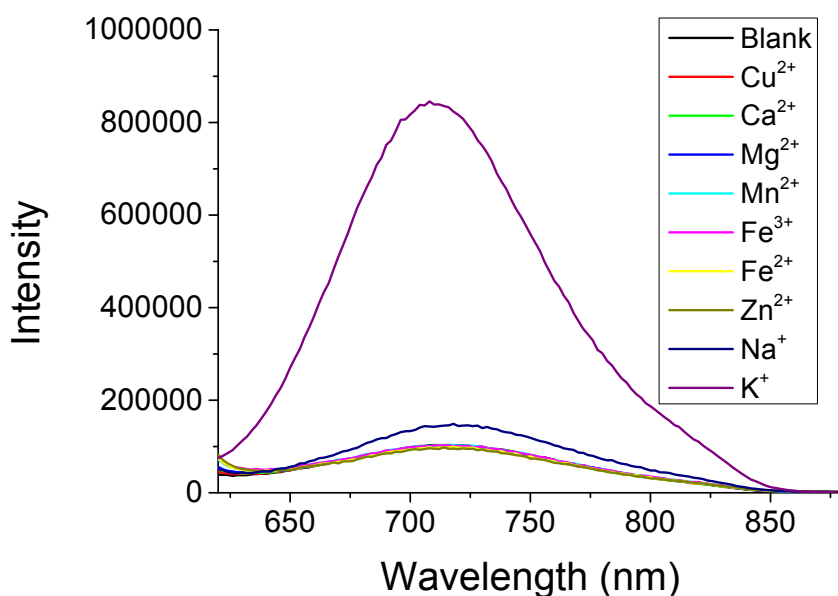


**Figure S6.** Fluorescence titration spectra of **TAC-Rh** (10  $\mu\text{M}$ ) containing different metal cations in HEPES buffer (pH 7.4, 5.0 mM)/CTAB (0.5 mM) solution. The ions are from  $\text{CuCl}_2$  (50  $\mu\text{M}$ ),  $\text{CaCl}_2$  (2.0 mM),  $\text{MgCl}_2$  (2 mM),  $\text{MnCl}_2$  (50  $\mu\text{M}$ ),  $\text{FeCl}_3$  (50  $\mu\text{M}$ ),  $\text{FeCl}_2$  (50  $\mu\text{M}$ ),  $\text{ZnCl}_2$  (2.0 mM),  $\text{NaCl}$  (15 mM), and  $\text{KCl}$  (200 mM) at intracellular physiological concentrations.

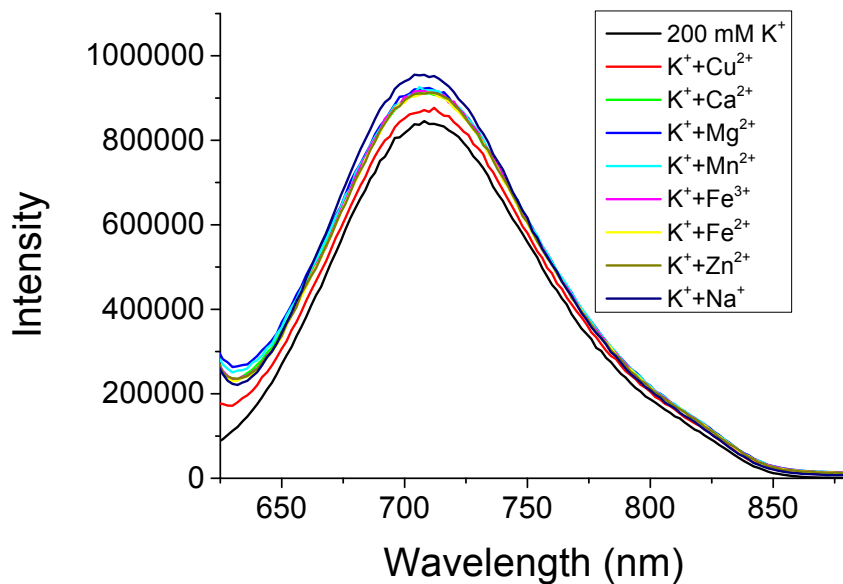


**Figure S7.** Fluorescence spectra of TAC-Rh-K<sup>+</sup> (200 nm) complex containing different metal cations in HEPES buffer (pH 7.4, 5.0 mM)/CTAB (0.5 mM) solution. The ions are from CuCl<sub>2</sub> (50 μM), CaCl<sub>2</sub> (2.0 mM), MgCl<sub>2</sub> (2 mM), MnCl<sub>2</sub> (50 μM), FeCl<sub>3</sub> (50 μM), FeCl<sub>2</sub> (50 μM), ZnCl<sub>2</sub> (2.0 mM), NaCl (15 mM), and KCl (200 mM) at intracellular physiological concentrations.

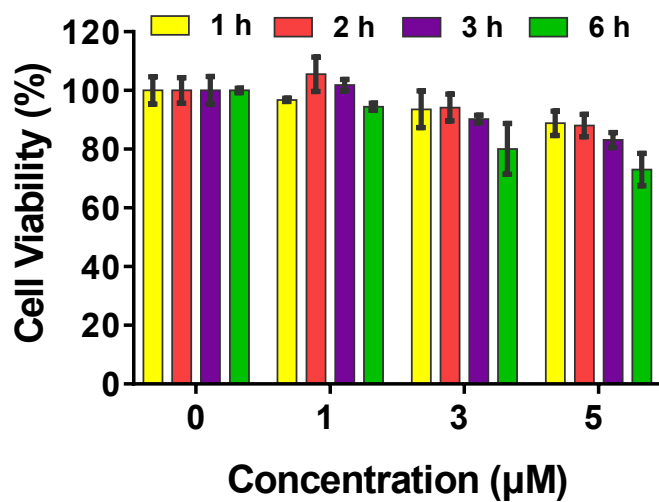
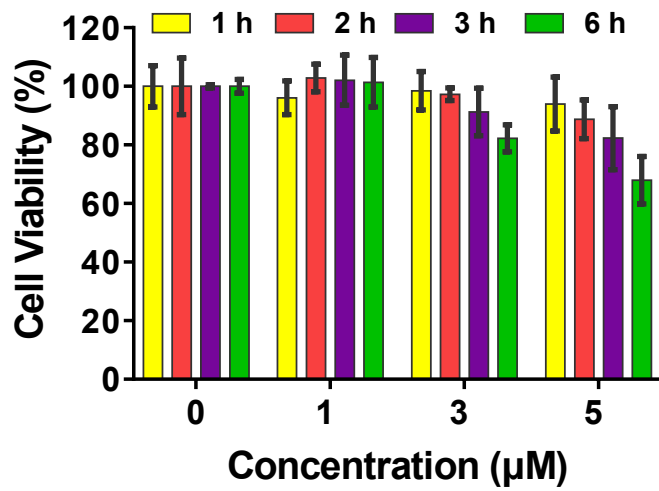
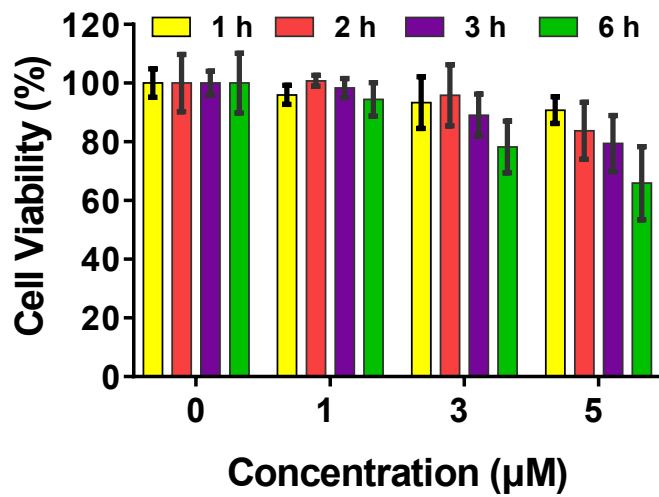


**Figure S8.** Cell viability test of (a) HeLa cells, (b) MDA-MB-231 cells, (c) MCF7 cells measured using the MTT assay for TAC-Rh at different concentrations and times.

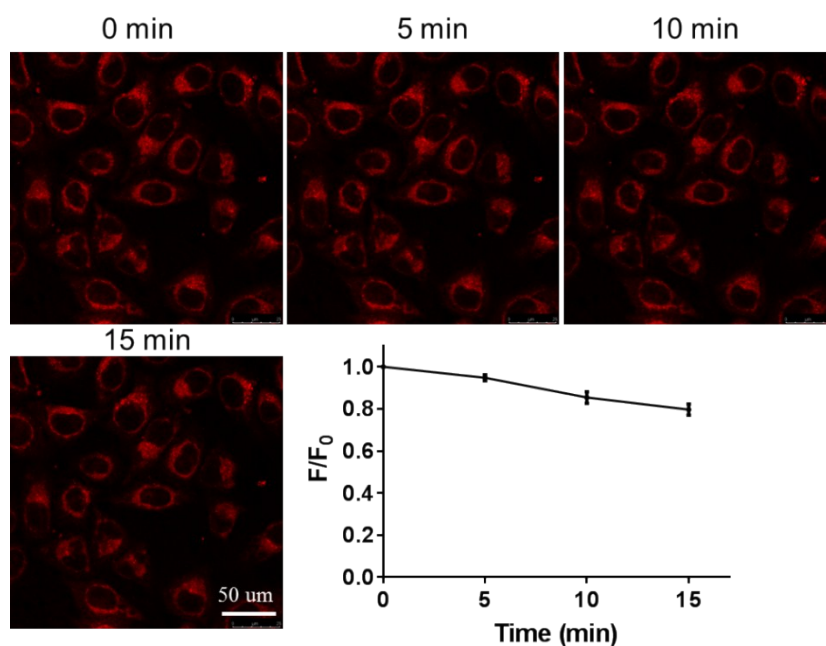


**Figure S9.** Time-dependent fluorescence images of HeLa cells. The average fluorescence intensity ratios as measured by Image J were shown in the graph.  $F_0$  is the average fluorescence intensity at  $t = 0$  min;  $F$  is the average fluorescence intensity at a given time point. The excitation wavelength and the emission wavelength ranges were 638 nm and 650-750 nm, respectively. And the following experiments in Figure S10-S19 were carried out in the same conditions.

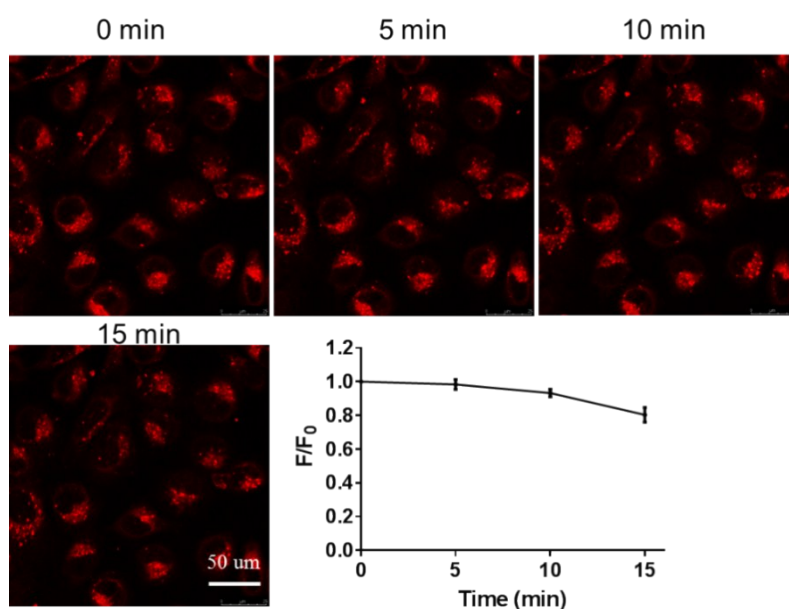


**Figure S10.** Time-dependent fluorescence images of TAC-Rh-stained MDA-MB-231 cells. The average fluorescence intensity ratios as measured by Image J were shown in the graph.  $F_0$  is the average fluorescence intensity at  $t = 0$  min;  $F$  is the average fluorescence intensity at a given time point.

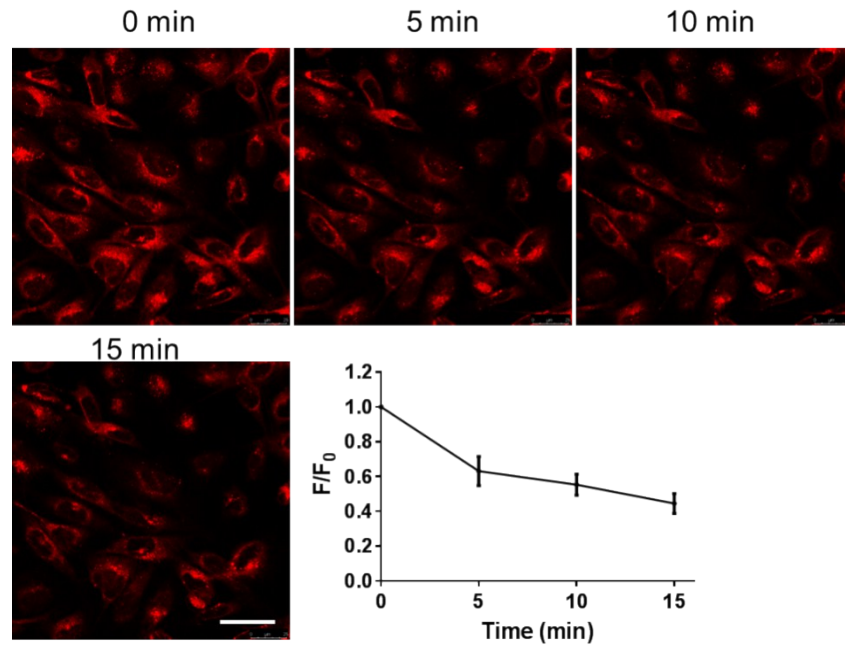


**Figure S11.** Time-dependent fluorescence images of TAC-Rh-stained MCF7 cells. The average fluorescence intensity ratios as measured by Image J were shown in the graph.  $F_0$  is the average fluorescence intensity at  $t = 0$  min;  $F$  is the average fluorescence intensity at a given time point.

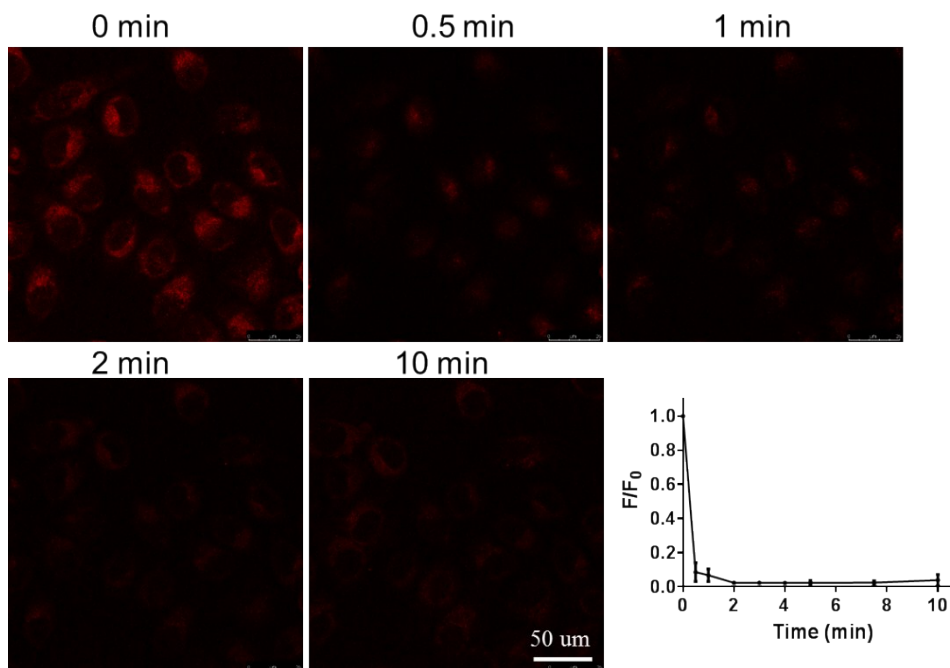


**Figure S12.** Time-dependent fluorescence images of HeLa cells after stimulation with ionomycin (10 mM). The average fluorescence intensity ratios as measured by Image J were shown in the graph.  $F_0$  is the average fluorescence intensity at  $t = 0$  min;  $F$  is the average fluorescence intensity at a given time point.

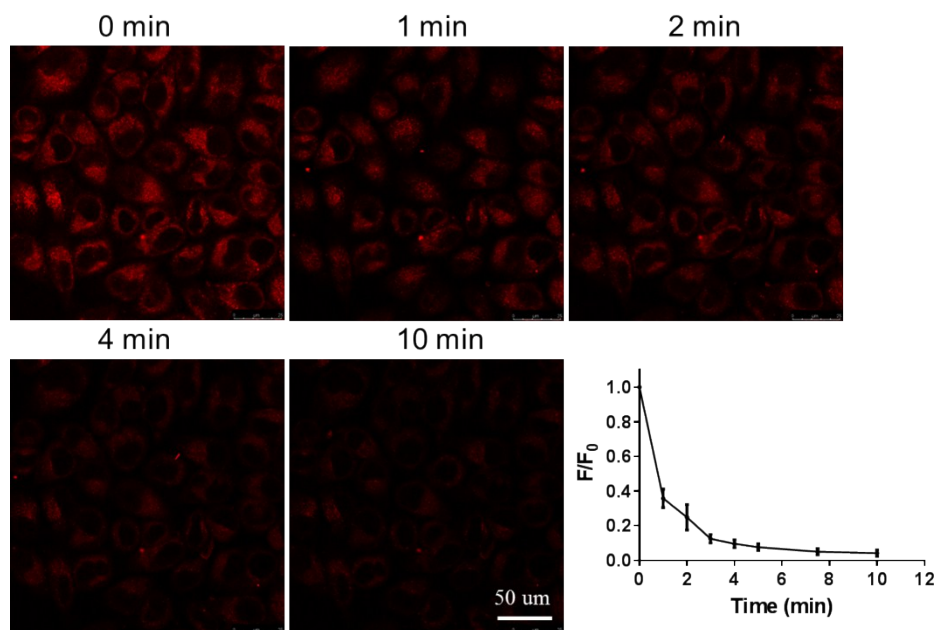


**Figure S13.** Time-dependent fluorescence images of HeLa cells after stimulation with nigericin (10 mM). The average fluorescence intensity ratios as measured by Image J were shown in the graph.  $F_0$  is the average fluorescence intensity at  $t = 0$  min;  $F$  is the average fluorescence intensity at a given time point.

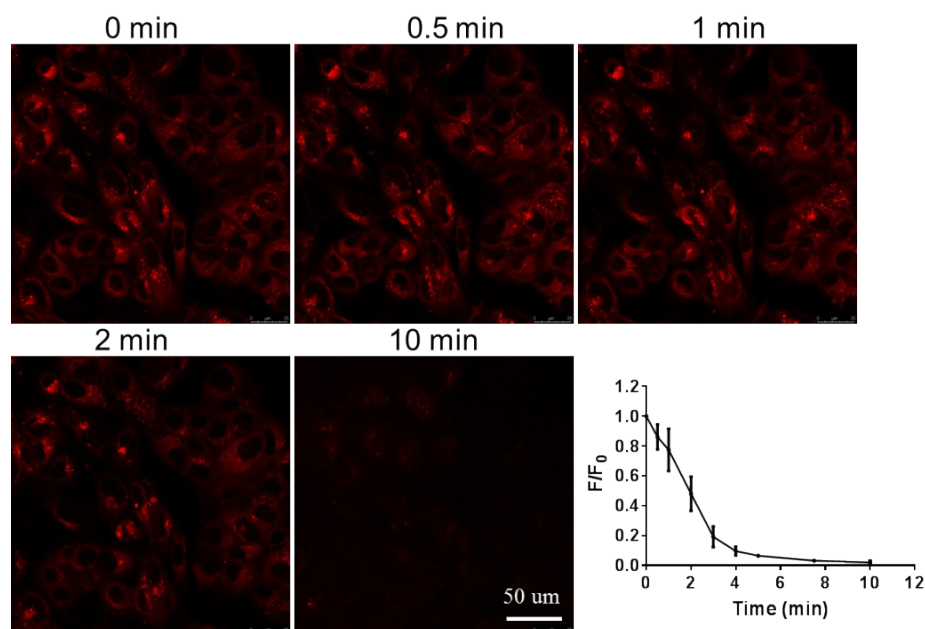


**Figure S14.** Time-dependent fluorescence images of MCF7 cells after stimulation with ionomycin (10 mM). The average fluorescence intensity ratios as measured by Image J were shown in the graph.  $F_0$  is the average fluorescence intensity at  $t = 0$  min;  $F$  is the average fluorescence intensity at a given time point.

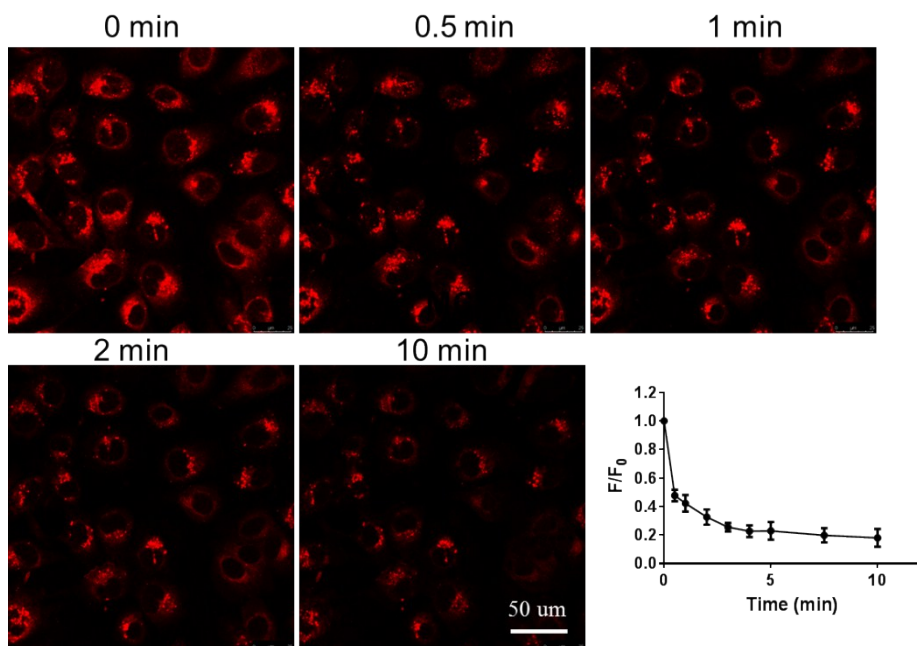


**Figure S15.** Time-dependent fluorescence images of MCF7 cells containing 200 mM of KCl after stimulation with ionomycin (10 mM). The average fluorescence intensity ratios as measured by Image J were shown in the graph.  $F_0$  is the average fluorescence intensity at  $t = 0$  min;  $F$  is the average fluorescence intensity at a given time point.

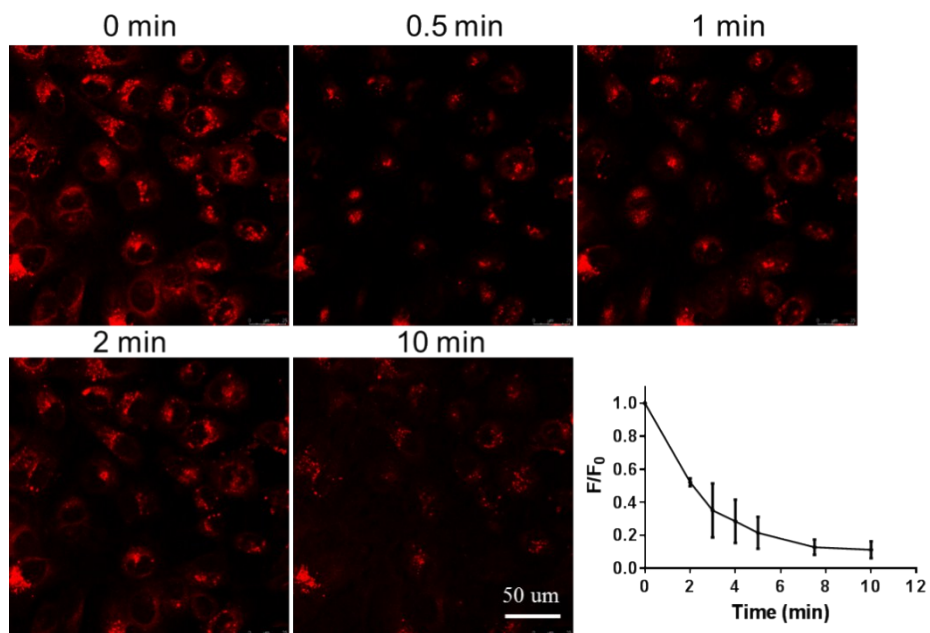


**Figure S16.** Time-dependent fluorescence images of MCF7 cells after stimulation with nigericin (10 mM). The average fluorescence intensity ratios as measured by Image J were shown in the graph.  $F_0$  is the average fluorescence intensity at  $t = 0$  min;  $F$  is the average fluorescence intensity at a given time point.

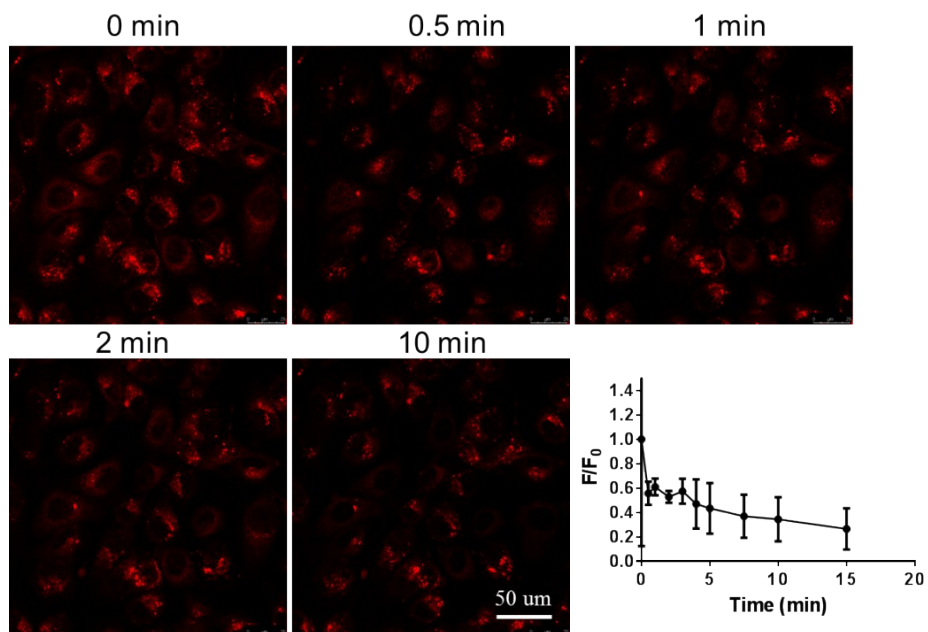


**Figure S17.** Time-dependent fluorescence images of MCF7 cells containing 200 mM of KCl after stimulation with nigericin (10 mM). The average fluorescence intensity ratios as measured by Image J were shown in the graph.  $F_0$  is the average fluorescence intensity at  $t = 0$  min;  $F$  is the average fluorescence intensity at a given time point.

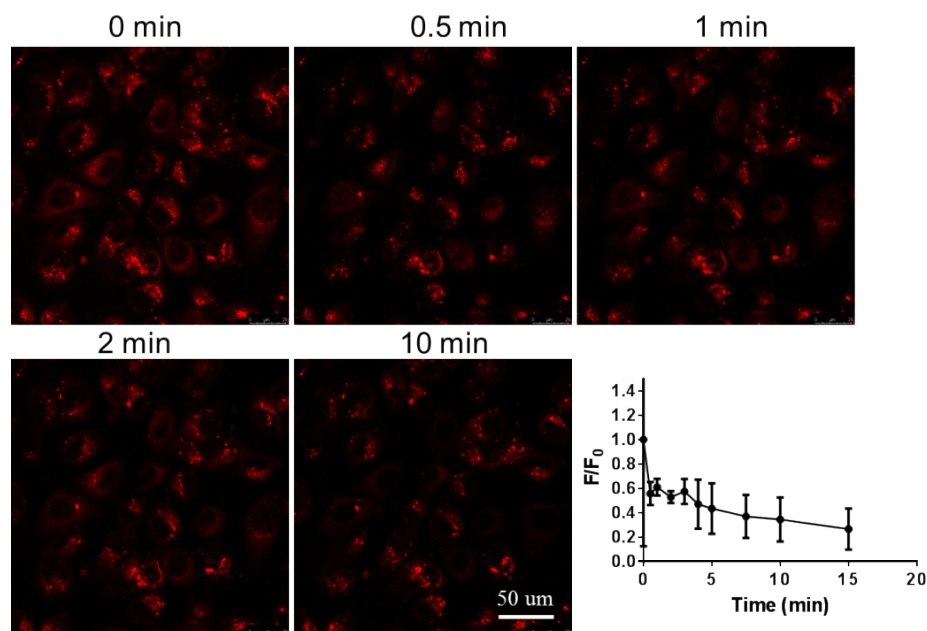


**Figure S18.** Time-dependent fluorescence images of MDA-MB-231 cells after stimulation with nigericin (10 mM). The average fluorescence intensity ratios as measured by Image J were shown in the graph.  $F_0$  is the average fluorescence intensity at  $t = 0$  min;  $F$  is the average fluorescence intensity at a given time point.

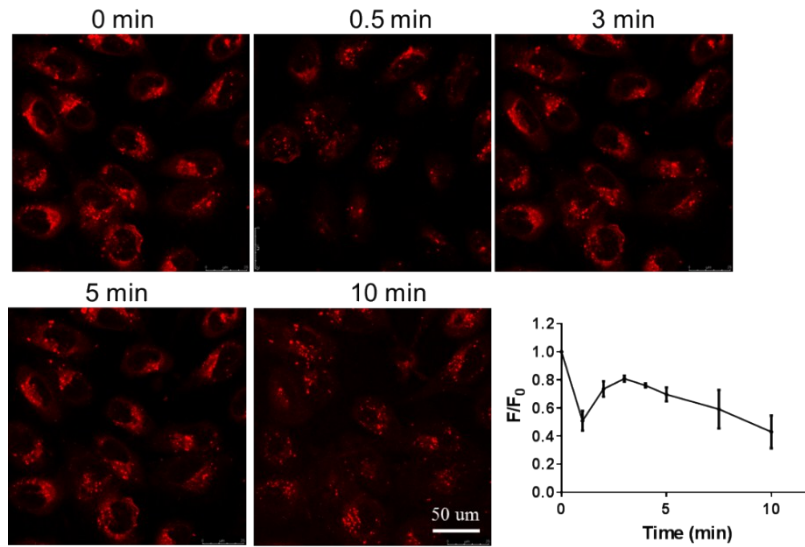


**Figure S19.** Time-dependent fluorescence images of MDA-MB-231 cells containing 200 mM of KCl after stimulation with nigericin (10 mM). The average fluorescence intensity ratios as measured by Image J were shown in the graph.  $F_0$  is the average fluorescence intensity at  $t = 0$  min;  $F$  is the average fluorescence intensity at a given time point.

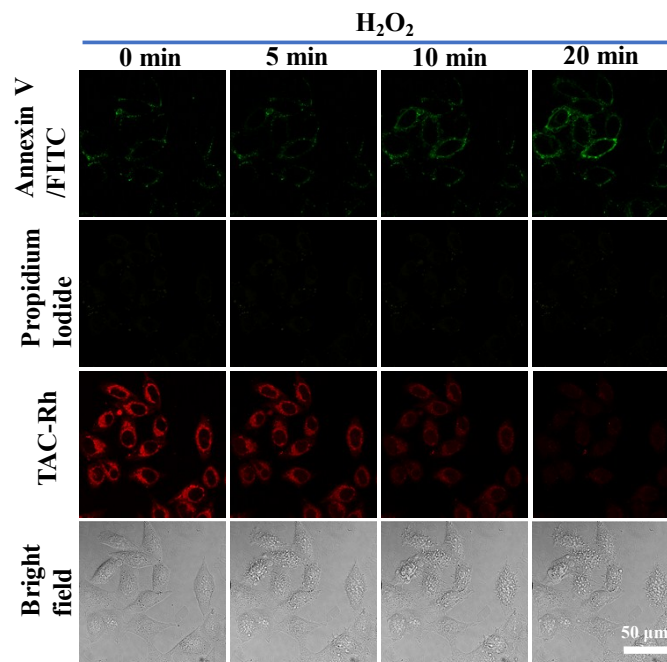


**Figure S20.** Time-dependent confocal fluorescence microscopy imaging of HeLa cells stimulated with  $H_2O_2$  (100 mM) stained with Annexin V/FITC, Propidium Iodide and TAC-Rh into culture medium. Excitation filter: 488 nm for Annexin V/FITC, 552 nm for PI, 638 nm for TAC-Rh; Emission: 493-540 nm for Annexin V/FITC, 600-650 nm for PI, 650-750 nm for TAC-Rh.

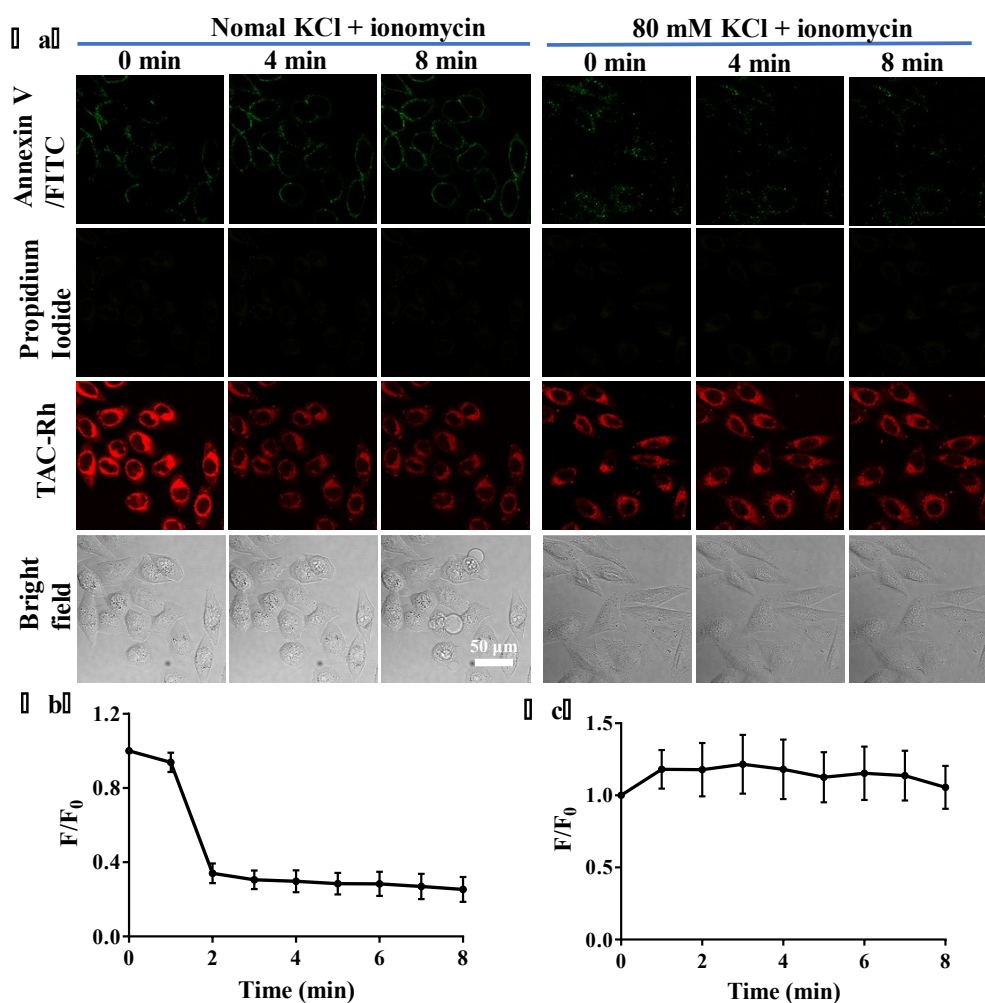


**Figure S21.** Time-dependent confocal fluorescence microscopy imaging of HeLa cells stimulated with ionomycin (20 mM) stained with Annexin V/FITC, Propidium Iodide and **TAC-Rh** in the normal culture medium and the culture medium containing 80 mM KCl (a). The average fluorescence intensity ratios of **TAC-Rh** in the normal culture medium (b) and in the culture medium containing 80 mM KCl (c) as measured by Image J were shown in the graph.  $F_0$  is the average fluorescence intensity at  $t=0$  min;  $F$  is the average fluorescence intensity at a given time point. Excitation filter: 488 nm for Annexin V/FITC, 552 nm for PI, 638 nm for **TAC-Rh**; Emission: 493-540 nm for Annexin V/FITC, 600-650 nm for PI, 650-750 nm for **TAC-Rh**.

#### References:

1. Kong X.; Su F.; Zhang L.; Yaron J.; Lee F.; Shi Z.; Tian Y.; Meldrum D. R., *Angew. Chem. Int. Ed.* 2015, **54**, 12053.
2. Zhang S.; Adhikari R.; Fang M.; Dorh N.; Li C.; Jaishi M.; Zhang J.; Tiwari A.; Pati R.; Luo F.; Liu H., *ACS Sens.* 2016, **1**, 1408.
3. Sui, B.; Yue, X.; Kim, B.; Belfield, K. D., *ACS Appl. Mater. Interfaces* 2015, **7**, 17565.
4. Zhou, X.; Su, F.; Tian, Y.; Youngbull, C.; Johnson, R. H.; Meldrum, D. R., *J. Am. Chem. Soc.* 2011, **133**, 18530.

5. Müller, B. J.; Borisov, S. M.; Klimant, I., *Adv. Funct. Mater.* 2016, **26**, 7697.
6. Bandara, H. M. D.; Hua, Z.; Zhang, M.; Pauff, S. M.; Miller, S. C.; Davie, E. A. C.; Kobertz, W. R., *J. Org. Chem.* 2017, **82**, 8199.